JOURNAL OF SPACECRAFT AND ROCKETS
Vol. 44, No. 1, January–February 2007

Chamber Core Structures for Fairing Acoustic Mitigation

Steven A. Lane,* Kyle Henderson,* and Andrew Williams†
U.S. Air Force Research Laboratory, Kirtland Air Force Base, New Mexico 87117-5776
and
Emil Ardelean‡
Science Applications International Corporation, Albuquerque, New Mexico 87106

DOI: 10.2514/1.17673

The U.S. Air Force Research Laboratory is pursuing an innovative composite structure design called chamber core for constructing launch vehicle payload fairings. A composite chamber core fairing consists of many axial tubes sandwiched between face sheets, tubes that can be used as acoustic dampers to reduce low-frequency interior noise with virtually no added mass. This paper presents the results of experimental studies of noise transmission through a 1.51 m diameter × 1.42 m tall chamber core cylinder. It was tested in a semireverberant acoustics laboratory using band-limited random noise at sound pressure levels up to 110 dB. The bare cylinder provided approximately 12.7 dB of attenuation over the 0–500 Hz bandwidth and 15.3 dB over 0–2000 Hz. The noise reduction increased to over 18 dB for both bandwidths with the axial tubes acting as acoustic dampers. Narrowband reductions in excess of 15 dB were measured around specific acoustic resonances. This was accomplished with virtually no added mass to the composite cylinder. Results were compared with the performance provided by a 2.5 cm acoustic blanket treatment. The acoustic dampers were as effective as the acoustic blanket at low frequency, but not at higher frequencies. The acoustic dampers were better able to couple with and damp the low-frequency acoustic modes. Together, the acoustic blanket and dampers provided over 10 dB more noise reduction over the 2000 Hz bandwidth than the bare cylinder.

I. Introduction

THE external acoustic loads experienced by a payload fairing can exceed 160 dB (the sound pressure level relative to 20 μPa) during launch. Noise and vibration transmitted into the fairing volume can damage sensitive payload components and poses a significant risk to payload launch survivability. Launch survivability drives the structural design and qualification of commercial, scientific, and military payloads. Composite payload fairings that are currently being studied by government and industry for both small and large launch vehicles are especially prone to excessive noise transmission. Low area density composite fairings allow for more payload mass, but also provide less protection against external launch noise. In addition to less mass, composite fairings typically have little inherent structural damping, which can also contribute to more structural–acoustic transmission.

Acoustic blankets and foam-type treatments are commonly used to mitigate noise in many enclosed-space situations, including payload fairings. However, attenuation of low-frequency acoustic resonances is challenging because acoustic blankets become less effective as the acoustic wavelength exceeds the thickness of the blanket. Therefore, more acoustic damping material is required to mitigate low-frequency noise, which adds weight to the fairing and reduces the amount of mass and volume available for the payload. Low-frequency acoustic resonances can be particularly problematic if they occur near structural resonances of the payload or payload components.

In addition to acoustic blankets, other approaches are being investigated for mitigating fairing noise. Some of the passive noise control approaches investigated by the U.S. Air Force Research Laboratory include damped Helmholtz resonators, composite blankets (incorporating distributed vibration absorbers), and a combined structural–acoustic damper called a "passive vibroacoustic attenuation device" [1–3]. In laboratory experiments, these approaches typically provided 6 dB of narrowband attenuation, and 2–3 dB broadband attenuation. Active control methods were also investigated both experimentally and in numerical studies [4–6]. The active control methods investigated include active structural–acoustic control (simulated optimal feedback control with piezoelectric actuators/sensors on a composite fairing), active acoustic damping with distributed sensor/actuator arrays (experimentally), and adaptive feedforward structural–acoustic control using distributed active vibration absorbers (experimentally). Performance of the active control systems was comparable to the performance of passive treatments, but the active systems were considerably more difficult to implement and introduced additional mass.

A chamber core structure uses axial composite tubes that are cured between wound inner and outer face sheets, forming a fairing structure as illustrated in Fig. 1a [7–9]. A chamber core fairing offers a strong yet lightweight structure. As shown in Fig. 1a, the fairing structure is essentially a "sandwich" composite, with axial "chambers" in the core. Figure 1b shows the vibroacoustic launch protection experiment (VALPE) (sounding rocket) fairing, which was the first chamber core fairing actually launched [10,11]. VALPE was a suborbital test that demonstrated several prototype payload protection systems, launched in 2003. Figure 1c shows the VALPE chamber core fairing integrated with the nose cone and aft support on its vibration test stand. An objective of this experiment was to investigate the feasibility of making fairings using the chamber core approach. The main focus was on design, fabrication, integration, and qualification of the first chamber core fairing; the acoustic protection provided by the fairing was secondary.

The axial tubes forming the core chambers and that provide such high strength-to-weight are not necessarily empty. In fact, testing was conducted on a small chamber core structure, shown in Fig. 2, to compare the noise reduction of an empty (bare) structure to the noise reduction measured using a variety of materials of different density and granularity to fill the chambers [12,13]. Results were intuitive; lightweight, loose granular fill provided some increased structural damping, but little overall acoustic reduction. As the density of the

Received 12 May 2005; revision received 26 October 2005; accepted for publication 17 December 2005.

*Senior Aerospace Engineer, Space Vehicles Directorate, 3550 Aberdeen Avenue. Member AIAA.
†Research Aerospace Engineer, Space Vehicles Directorate, 3550 Aberdeen Avenue. Member AIAA.
‡Acoustics Engineer, 2109 Air Park Road. Member AIAA.

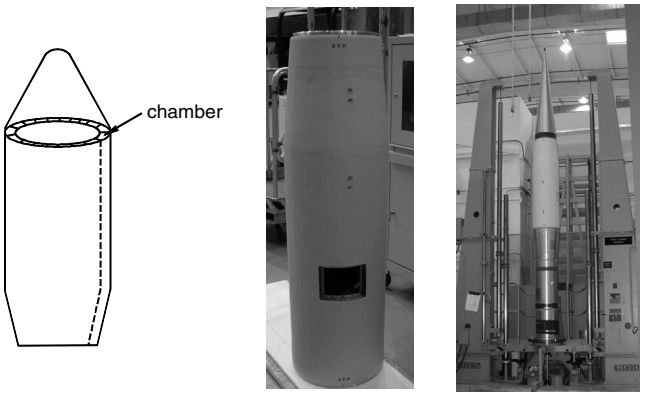

a) b) c)

Fig. 1 Illustration of chamber core fairings: a) schematic; b) VALPE fairing; c) integrated VALPE fairing during qualification testing.

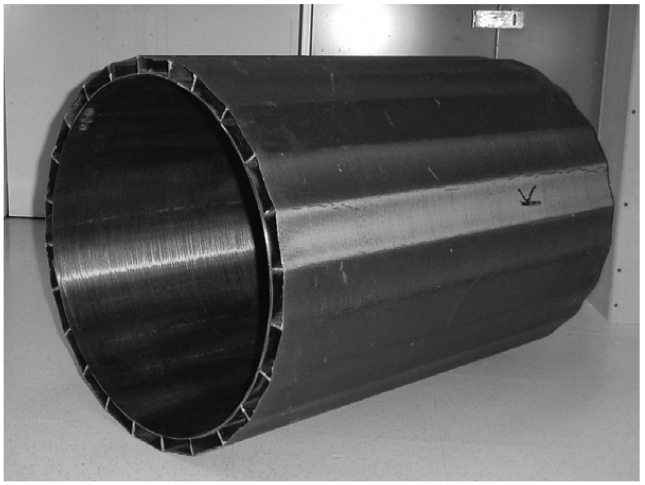

Fig. 2 Early chamber core structure used for noise reduction experiments.

fill material increased, the additional mass provided more noise reduction at high frequency. There was virtually no benefit at low frequency. In a different test, the chambers of a larger Kevlar-epoxy chamber core cylinder were filled with water, which provided an order of magnitude reduction (20 dB) of the measured noise transmission (10 Hz–5000 Hz), most of which occurred above 200 Hz. However, the weight of the water plus that of the chamber core structure was more than an order of magnitude greater than the weight of the bare cylinder alone.

Acoustic resonators (or acoustic "dampers" if the resonators are made resistive as opposed to reactive) have proven feasible for damping low-frequency acoustic resonances in many applications. Thus, it is obvious to ask if the axial tubes of the chamber core fairing can be made to act as acoustic dampers, coupling with and attenuating the interior acoustic resonances of the payload volume. Conceptually, this would be accomplished by boring an orifice through the inner face sheets into the chamber core tube. The fairing structure itself then acts as multiple "organ pipe" resonators, which can be tuned to cover a broad frequency bandwidth. The chamber core fairing would not actually decrease noise transmission, but rather increase acoustic damping (particularly at low frequencies), and thereby decrease the interior acoustic response. This is the primary focus of the work presented here.

This paper first presents essential theoretical background on the fairing noise control problem and the physics underlying the implementation and modeling of axial, chamber core acoustic dampers. The development of an appropriate test method and apparatus to evaluate the acoustic performance of a chamber core structure is discussed. Experiments performed on a graphite–epoxy chamber core cylinder are presented, and results from implementing the acoustic dampers with a 2.5 cm acoustic blanket treatment are compared and discussed.

II. Theory

A. Fairing Noise Transmission Dynamics

The primary source of payload fairing noise is the rocket exhaust plumes. The sound produced tends to be broadband, and propagates up the side of the launch vehicle fairing as plane waves at sharp oblique angles of incidence. Each rocket plume is an independent, uncorrelated acoustic source. The noise from the exhaust plume will typically be directional, often originating from launchpad exhaust ducts; therefore, coupling with the fairing will be asymmetric, an important consideration for simulations. The fairing's internal acoustic response can be described as the result of the disturbance being filtered by a strongly coupled system composed of the fairing and the enclosed acoustic volume. Transmission is governed by the coupling of the external acoustic field with the structure, the dynamic response of the structure, the coupling of the structural response to the acoustic volume, and the dynamics of the acoustic volume.

Gardonio et al. [14] provide an excellent analytical analysis of structural–acoustic transmission for a cylinder that is very much applicable to the fairing noise problem. Their paper presented the development and application of a modal-interaction analysis to investigate plane-wave transmission of external noise into a representative model of a cylindrical, sandwich composite fairing. They developed a coupled structural–acoustic model assuming weakly coupled, in vacuo structural modes and rigid-wall acoustic modes. They discussed the effects of structural mass, stiffness, and damping on the coupled structural–acoustic response, and presented the impact of "blocking masses" to reduce noise transmission through a fairing. Simulation results showed the importance of the angle of incidence on determining the coupling coefficient between the structural and acoustic subsystems. They demonstrated how the structural–acoustic system "filters" the external disturbance. Their results showed that simply adding mass to the fairing (i.e., increasing the area density) affected the noise reduction above 100 Hz (not always beneficially), but had little effect below 100 Hz. Another important point that they demonstrated was that poor noise reduction occurred at frequencies where structural modes and acoustic cavity modes exhibited good "spatial coupling" and good coupling with the external field.

A simply supported right circular cylinder, as presented by Gardonio, provides a reasonable test bed to investigate fairing noise transmission. For chamber core structures, it is much easier to fabricate a cylinder as opposed to a tapered fairing. The test structure investigated in this work is shown in Fig. 3. The 1.51 m diameter $\times$ 1.42 m length cylinder was fabricated from graphite–epoxy composite. Multilayer particle-board/foam end-caps were designed to exhibit low transmission, so that the primary transmission path would be the cylinder. The structure was designed to be traceable to an actual fairing design; that is, comparable strength-to-weight, wall thicknesses, composite layup, and area density. The system was sealed as much as practical to prevent flanking paths, but some leakage was unavoidable (for cabling ports and microphone-boom fixtures).

The acoustic resonances of the test cylinder were computed using a rigid-wall model of the acoustic volume and are given in Table 1 ($\pm$0.5 Hz) [15]. The actual acoustic resonances of the cylinder were observed in measured frequency response functions (FRF) between a small speaker placed inside the cylinder and several microphones placed throughout the inside of the cylinder ($\pm$0.5 Hz). A small accelerometer [PCB Model 352C22, sensitivity = 1 mV/(m/s/s), mass = 0.5 g, dynamic range = 1 Hz to 10 kHz] attached to the speaker's diaphragm provided a reference signal for the FRF measurements, and the speaker was driven with band-limited random noise. Some of the measured FRFs are given in Fig. 4. Table 1 compares the measured acoustic resonance frequencies to the computed frequencies. Matching was good up through 300 Hz. Because the disturbance source and sensors were both inside of the

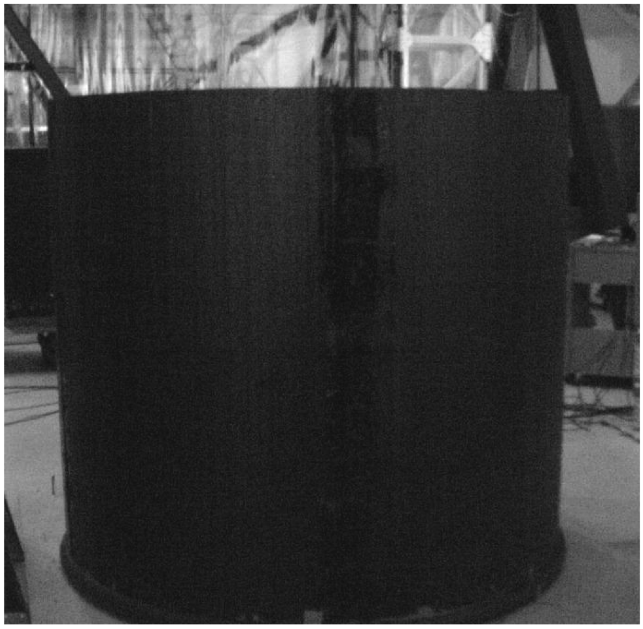

Fig. 3 The chamber core test article.

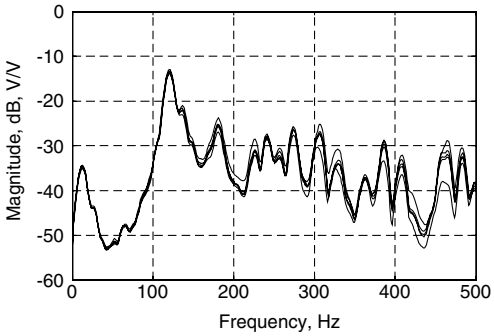

Fig. 4 Representative FRFs for interior acoustic measurements.

cylinder, there was virtually no coupling with the structural modes. The first acoustic resonance (at about 120 Hz) was very pronounced in Fig. 4. The peak at low frequency (12 Hz) is the "Helmholtz mode," also known as the "breathing mode" or "0 Hz" acoustic mode. It is not 0 Hz due to small leaks in and around the cylinder end caps, particularly at the sensor/actuator cable port, which allowed air to flow in and out of the cylinder's interior volume, much like what happens in a Helmholtz resonator. The frequency of this breathing mode is a function of the "leakage"; if the cylinder was perfectly sealed, then the resonance frequency would be identically zero.

Structural modeling of the test article was not performed because the structural properties were not accurately quantified during fabrication, the composite layup was not consistent over the entire surface area, and boundary conditions were not well defined. Although it may have been an interesting challenge to develop and validate a structural model, it was not essential for the present study, and likely would have been a daunting task.

Table 1 Predicted and measured acoustic resonances of the cylinder volume

Resonance	Measured, Hz	Predicted, Hz
1	120	121
2	137	136
3	181	182
4	225	225
5	241	242
6	257	256
7	274	277
8	303	283
9	306	307

B. Cavity and Resonator Coupling

Figure 4 shows that the acoustic resonances were very lightly damped across the 0–500 Hz bandwidth. Acoustic dampers (resonators) can be used to damp cavity modes in the same way that tuned mass dampers can damp vibrations on structures. Fahy and Schofield studied the interaction of a single acoustic (room) mode and a single acoustic resonator, and performed experiments to examine optimal tuning and attenuation [16,17]. They showed that the optimal damping for narrowband attenuation of a single acoustic mode can be expressed as

$$\frac{\varepsilon}{\eta_n} = \frac{2(\frac{\varepsilon}{\eta_r})^3}{1 - (\frac{\varepsilon}{\eta_r})^2 - (\frac{\varepsilon}{\eta_r})^4} \tag{1}$$

where ε is the coupling parameter, η_n is the acoustic modal damping of the cavity (room) mode, and η_r is the damping of the acoustic resonator. The coupling between the resonator and the acoustic cavity is given as

$$\varepsilon^2 = \frac{\rho_0 c_0^2 \varphi_n^2(\boldsymbol{r}_r) S^2}{\omega_c^2 \Lambda_n M} \tag{2}$$

where M/S^2 is the acoustic mass of the system, ω_c is the resonance frequency of both the acoustic mode and the additional resonator, ρ_0 is the density of the fluid, c_0 is the sound speed of the fluid, Λ_n is the modal volume of mode n, and $\varphi_n(\boldsymbol{r}_r)$ is the value of the mode shape function for mode n at the resonator neck. Their results showed that for a coupled resonator/acoustic system, the effect of the resonator was to split the acoustic resonance of the cavity into two resonance peaks that occurred on either side of the original acoustic resonance frequency. The magnitude of the resulting two peaks was typically less than that of the original. It is apparent in Eq. (1) that strong coupling can occur only in modes in which the resonator neck (or orifice) is not located at a pressure node, as that would result in the value of the mode shape going to zero.

Cummings expanded this work to a multimode acoustic system and analyzed the effects of multiple resonators using numerical simulations [18]. He addressed the issue of coupling to multiple acoustic modes with a single acoustic resonator. His research showed that in high modal density acoustic systems, a single resonator was able to couple with multiple resonances. Furthermore, Cummings observed that for widely spaced acoustic modes (i.e., separated by a range of frequencies so that each mode is clearly distinguishable), two resonators designed for different modes have little influence upon each other. The reason was that the impedance of a single resonator becomes large away from its resonance frequency, and therefore couples weakly to the acoustic field or other resonators.

In addition to the position of the resonator orifice relative to the acoustic pressure nodes (i.e., spatial coupling), Eq. (1) indicates the strong dependence of resonator performance on the damping of the resonator and the acoustic system. It has been noted that a resonator will split an acoustic resonance peak into two lesser amplitude peaks. However, if damping is added to the resonator, the two resulting peaks can be further reduced in amplitude, creating a smooth plateau effect referred to as "optimal" by Fahy. However, excessive damping can reduce coupling, thereby reducing performance. Cummings noted that for lightly damped resonators (reactive), the level of reduction of a target acoustic resonance was sensitive to room-mode damping. If the room mode was significantly damped, then little benefit could be gained by adding a resonator/damper. For constant resonator damping, the level of achievable reduction of the target room mode increased as the damping of the room mode decreased. Therefore, large levels of reduction can be achieved only if the room mode is initially lightly damped. In such cases, a resistive resonator may provide more optimal results than a reactive resonator (there is inherent damping in acoustic resonators that results from radiation

losses and viscous effects in the neck). Another important conclusion was that as resonator damping increased (becoming resistive), the sensitivity of the resonator's performance to mistuning was reduced. The room mode analysis presented by Fahy and Cummings is directly applicable to payload fairings, which often have lightly damped, low-frequency, widely spaced cavity resonances as shown in Fig. 4.

C. Acoustic Damper Modeling and Testing

A reasonably accurate model of the acoustic damper is necessary so that the "as built" damper effectively couples with the target cavity resonance. The axial resonators of a chamber core structure do not follow the classic lumped-parameter, Helmholtz resonator model given as

$$\omega_n = c_0 \sqrt{\frac{S}{L_n V}} \tag{3}$$

where c_0 is the sound speed, S is the neck cross-sectional area, L_n is the effective neck length, and V is the resonator cavity volume. Helmholtz resonators typically have an acoustic wavelength ($\lambda = 2\pi c_0/\omega_n$) longer than any dimension of the resonator, but in the case of chamber core tubes, the desired wavelength of the resonator may approach the length of the tube. It was shown by the authors that such acoustic resonators behave more like "quarter-wave" resonators [19] than classical Helmholtz resonators. To investigate, several "tube resonator" designs were built from polyvinyl chloride (PVC) pipe and tested, including the one shown schematically in Fig. 5. The design of these tube resonators (particularly, the cross-sectional area) was intended to mimic the chamber core fairing axial chambers. Analysis of the experimental data showed that the fundamental resonance frequency of such resonators is reasonably predicted by

$$f_1 = \frac{c_0}{4L_{\text{eq}}} \tag{4}$$

where L_{eq} is calculated as

$$L_{\text{eq}} = \alpha L_n + \beta L_2 \tag{5}$$

with c_0 being the sound speed, and α and β the model parameters. The length denoted as L_1 was not needed to model the first acoustic resonance. Instead of an analytical expression for parameters α and β, both were determined empirically by curve fitting experimental data from a variety of tube configurations (varying diameters and geometry). Initially, the tubes were tested in a free field and an appropriate model computed to fit the measured resonance frequencies (least-squares curve fit). Figure 6 presents the measured resonance frequencies and the corresponding "curve fit" model for a single test series, where $L_1 + L_2 = 80$ cm, with L_n ranging from 6 to 18 cm, all with 13 mm diameters. For this particular case, it was determined that $\alpha = 1.9$ and $\beta = 0.9$. The comparison demonstrates that the model offers reasonably good correlation with experimental data.

Each tube was then tested in a reverberant aluminum cylinder (50 cm diameter × 2.1 m length) to observe the impact of coupling between the resonator and the acoustic cavity. The results indicated that significant coupling did occur, and that design parameters α and β must be measured in situ for a particular resonator design. However, it was desired to predict the behavior of the actual chamber core tubes before having cut any holes in the test structure. Therefore, once the composite test article was fabricated, more PVC tubes, such as the one shown in Fig. 5, were fabricated and attached to the inside of the cylinder. With the chamber core cylinder capped and sealed, the parameters α and β were determined for a range of PVC tube lengths (L_1, L_2, and L_n). A total of 20 resonators were tested. The inner diameter of the tubes was 2.86 cm (1.125 in.), so that the cross-sectional area was approximately equal to that of the chamber core tubes. The diameter of the neck was chosen to be 1.9 cm (0.75 in.). Four tube lengths (L_2), ranging from 0.87 to 1.32 m, with five neck lengths (L_n), ranging from 5 to 15.2 cm were tested. Fundamental frequencies were measured for each tube, and using Eqs. (5) and (6), the two design parameters were calculated as $\alpha = 2.59$ and $\beta = 0.99$. The sound speed was assumed to be about 336 m/s (23°C at 1620 m above sea level). This provided a guideline for developing the actual axial chambers into acoustic dampers of the desired frequency without having to "blindly" bore holes into the cylinder.

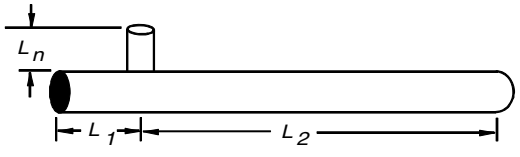

Fig. 5 Illustration of a tube resonator.

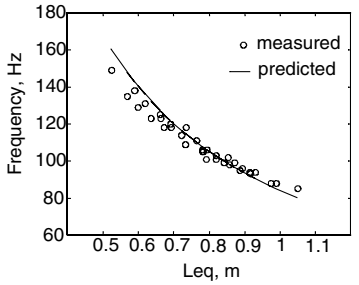

Fig. 6 Model predictions versus experimental measurements for the resonator shown in Fig. 5 ($L_1 + L_2 = 80$ cm).

Prior testing on an aluminum cylinder using PVC tube resonators demonstrated that single and multiple cavity modes could be attenuated using a multiresonator configuration as predicted by Cummings [18]. It was also observed that optimal coupling between the cavity modes and acoustic dampers occurred with the resonator necks positioned near the ends of the cylinder near the rigid-wall boundaries, as one would expect by examining the structural and acoustic mode shapes. For the aluminum cylinder, the inherent damping of the tube resonators appeared to provide effective coupling and reasonable performance.

For the tests conducted on the chamber core cylinder, it was desired to design the chamber core resonators to cover an entire bandwidth, from about 55–2000 Hz, in nearly equally spaced increments. This was thought reasonable based on the numerical studies of Cummings, and prior work using the aluminum cylinder. To accomplish this, the axial chambers (180 total) were designed to have carefully spaced resonance frequencies over the target bandwidth. It was decided to divide the chamber core into four regions, or quadrants. Tests on the aluminum cylinder demonstrated that having multiple resonators at the same frequency increased the attenuation of the target cavity mode. In each quadrant, one tube was used to form a single damper having a fundamental frequency of approximately 55 Hz, which corresponded to a key transmission peak (not an acoustic resonance). Because the length of the chamber core was 1.4 m, it was possible to transform the other 44 tubes of each quadrant into dual acoustic dampers by inserting foam plugs within each tube (the foam expanded and rigidized to form an airtight seal between the two chamber sections). This permitted a total of 88 different acoustic damper frequencies per quadrant, designed to cover the 60 to 2000 Hz bandwidth. A schematic of how this was implemented is given in Fig. 7. Most of the damper frequencies were below 200 Hz. The necks for each damper were located approximately 5 cm from the end caps. The foam plugs added some weight and structural damping, and so baseline measurements were taken to quantify this effect.

For actual applications, the acoustic dampers would be used only for low-frequency noise reduction (below 200 Hz), with acoustic blankets primarily used for higher frequency noise reduction. Acoustic blankets in the fairing increase the absorption within the fairing, which adds to the overall "noise reduction" provided by the cylinder/damper/blanket system. However, the added absorption would impact the optimal damper design and the benefits provided

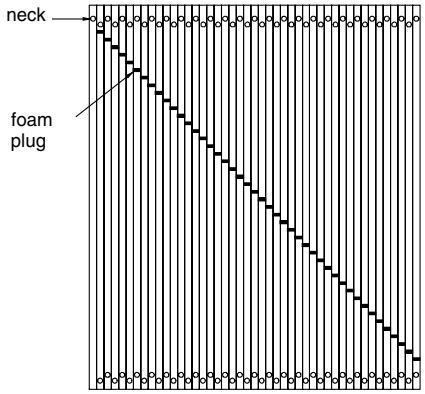

Fig. 7 Schematic of acoustic damper and plug layout for a single quadrant (45 axial chambers).

by the acoustic dampers (resonators). Therefore, tests were conducted to measure the performance of the chamber core structure with and without an added 2.5 cm acoustic (melamine) blanket attached to the cylinder interior. The acoustic blanket covered most of the interior surface area (5.4 m^2, $\approx$1.22 kg).

D. Measuring Performance

It was desired to quantify the performance of the chamber core structure, the effect of the acoustic dampers, and the combined effect of the dampers with the acoustic blanket treatment. The bandwidth of interest was up to 2000 Hz, and external sound pressure levels around 100–110 dB (re: 20 μPa) were considered adequate. For this program, testing was conducted in a large, semireverberant laboratory, using an array of speaker equipment [four 46 cm (18 in.) subwoofers, twelve 25 cm (10 in.) woofers, and six 13 cm (5 in.) midrange speakers driven by six high-power amplifiers] to provide the external disturbance over two test bandwidths: 0–500 Hz, and 0–2000 Hz (although 40 Hz was the approximate roll-off frequency of the subwoofers). The disturbance field was generated by a Siglab spectrum analyzer using band-limited random noise over two bandwidths, and crossover/equalizer equipment was used to shape the disturbance field. The laboratory was constructed from concrete and cinder block walls, and included many scattering surfaces that produced an approximate diffuse disturbance loading on the cylinder (i.e., no obvious room modes in the test bandwidths). This approach was chosen because a laboratory environment was more controllable and the experiments were more repeatable (thus reducing measurement uncertainty) than if they had been conducted outdoors. Although an outdoor test would arguably be more realistic, repeatability was a concern. Because a prime objective of this program was to study the noise reduction provided by various acoustic treatments and configurations, a consistent disturbance loading was desired. The approximate diffuse disturbance load created a more spatially even loading, preventing "hot spots," which might bias the transmission measurements.

Noise transmission and acoustic damper performance were measured by computing the "noise reduction," which is defined here to be the difference in the spatially averaged external sound field impinging on the cylinder and the spatially averaged interior acoustic response. Acoustic transmission through flat panels is typically measured using "transmission loss," but this quantity is not reasonable for a closed cylinder [20]. Noise reduction (NR) was computed over each bandwidth using the expression

$$\text{NR (dB)} = 20\log_{10}\left(\frac{\text{external rms}}{\text{internal rms}}\right) \tag{6}$$

which is similar to that presented by Bies, except here the transmission loss and absorption are combined into one metric [21].

To estimate the "external rms," a large sampling of the external sound field was taken around the circumference of the cylinder for each test. Microphone (PCB Model 130C10, sensitivity = 21.6 mV/Pa, dynamic range = 20 to 7000 Hz$\pm$ 1 dB, linearity$\langle 3\% \rangle$128 dB SPL) measurements were taken at 36 locations around the cylinder at approximately 7.5 cm (3 in.) from the outer surface. Time histories of the microphone signals for each position and test case were measured and stored. The time histories were high-pass filtered (4th order Butterworth, cutoff frequency of 20 Hz) in MATLAB [22] to remove any dc coupling and converted from voltage to the equivalent sound pressure (Pa). The rms of each signal was computed in both the time domain and in the frequency domain. The time-domain computations were straightforward. The time-domain rms values of each microphone position were averaged to yield an overall spatial average. For frequency-domain computations, the MATLAB command "pwelch" was used to compute the one-sided power spectral density (PSD) from each time history. The overall rms value was computed from the spatially averaged power spectral density function. Time-domain computations were compared with frequency-domain computations to verify agreement.

The "internal rms" was estimated using a microphone boom with 6 attached microphones (PCB Model 130C10, sensitivity= 21.6 mV/Pa, dynamic range = 20 to 7000 Hz $\pm$ 1 dB, linearity $\langle 3\% \rangle$128 dB SPL). The microphone boom was maneuvered inside the cylinder through a port through the top end cap. A total of 120 measurements were made at several positions along the length of the cylinder and at different rotation angles to adequately sample the internal response. The measurements were spatially averaged using the same time-domain and frequency-domain methods discussed for the external measurements.

III. Test Article and Experimental Setup

A. Chamber Core Cylinder

The cylinder consisted of 180 nearly square tubes (2.5 $\times$ 2.5 cm) by 1.42 m long tubes, sandwiched between inner and outer facesheets to form a 1.51 m diameter cylinder. A close-up view of the chamber core structure is presented in Fig. 8. Orifices were bored into each axial tube for attachment of resonator necks approximately 5 cm from the cylinder end. The centers of sequential orifices were offset by about 1.5 cm to allow sufficient clearance for attachment of the necks. No additional damping material was added to the acoustic resonators, as the inherent damping in the chambers seemed to provide good coupling and dissipation.

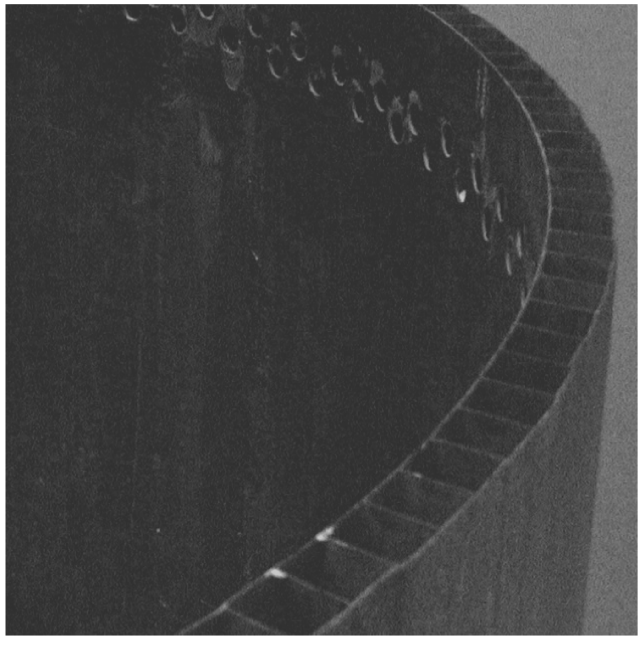

Fig. 8 Close-up view of the graphite–epoxy chamber core cylinder.

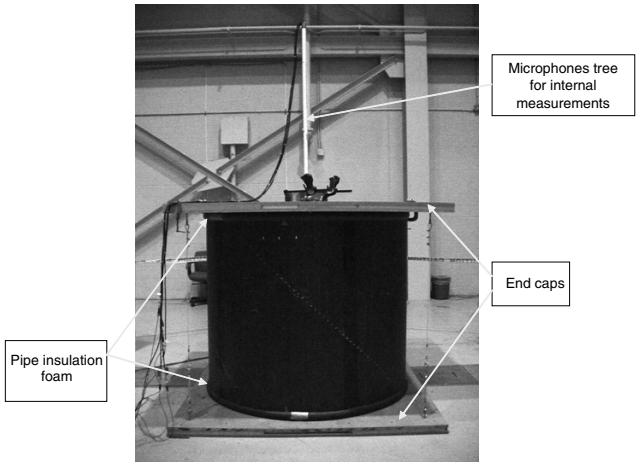

Fig. 9 Composite cylinder with end caps and microphone booms.

B. End-Cap Fabrication

The test article was placed between two heavy end caps of high acoustic impedance, as shown in Fig. 9, to create an acoustic enclosure for which the chamber core cylinder was the dominant transmission path (preventing flanking through the end caps). Each end cap consisted of a 2 cm layer of foam rubber sandwiched between two sheets of 2 cm medium density particle board. Firm contact between the end caps and the chamber core was ensured by using four tie rods. Tension in the tie rods was controlled with turnbuckles, one for each rod. A ring of 2 cm foam rubber (pipe insulation) was fitted around the circumference of each end of the cylinder to form a tight seal between the cylinder and the end caps. Cables for the internal microphones were brought out through the microphone-boom support structure. The boom support structure was fitted through the top end cap. Although great attention was given to reducing flanking paths, the enclosure was not completely sealed.

IV. Results

The first set of measurements compared the spatially averaged external response to the spatially averaged internal response for the bare chamber core cylinder. Figures 10 and 11 present the power spectral density plots for the 500 and 2000 Hz bandwidths, respectively. The data were taken early in the program before any plugs were inserted into the axial tubes or any orifices bored into the cylinder. The data indicated that the noise reduction of the bare cylinder was 12.7 dB for 0–500 Hz, and 15.3 dB for 0–2000 Hz. Measurement uncertainty for these and subsequent measurements was less than ± 0.2 dB, based on measurement repeatability and sensor uncertainty. In both cases, the external disturbance was relatively flat across the bandwidth except for the roll-off at low frequency that resulted from subwoofer roll-off. The Helmholtz mode is observable at approximately 30 Hz in the internal response shown in Fig. 10 (first peak on the far left). The same plot indicates a peak in transmission at approximately 55–60 Hz, which corresponds to a strongly radiating structural resonance. At the first acoustic resonance, about 120 Hz, there was a sharp increase in the internal acoustic response. Above the first acoustic resonance and up through 1000 Hz, there were many sharp peaks in the internal spectrum, indicative of lightly damped structural and acoustic resonances. At some frequencies, the interior response level was nearly equivalent to the external disturbance. Above 1000 Hz, there was more separation between the "trends," or average, of the internal and external responses. Although the PSD data were not divided by a reference pressure, the sound pressure levels (SPL) given in the subsequent figures are all relative to a reference pressure of 20 μPa.

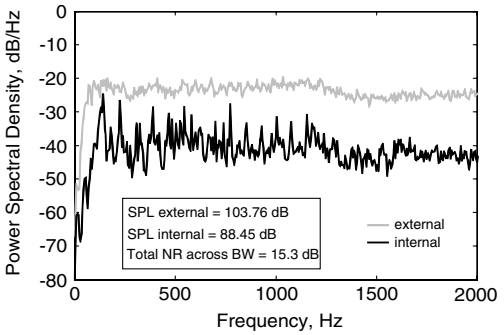

Fig. 11 External and internal noise levels for the bare cylinder (0–2000 Hz).

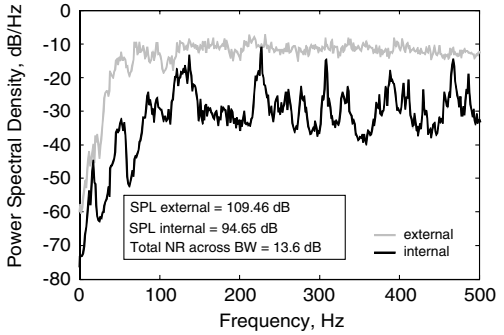

Fig. 12 External and internal responses with plugs added, but no acoustic dampers (0–500 Hz).

In the next series of tests, the plugs used to separate each tube into two acoustic dampers were inserted (as illustrated in Fig. 7). The added mass of the plugs was approximately 3% of the empty cylinder mass. The impact of the added mass is shown in Figs. 12 and 13, and forms the "baseline" for comparison of subsequent results. Overall, the noise reduction increased by 0.9 dB (over the 500 Hz bandwidth) and 0.7 dB (over the 2000 Hz bandwidth). Although the Helmholtz mode was more predominant ($\approx$5 dB), it did not impact the overall performance significantly. Structural transmission was more predominant at 55 and 90 Hz in Fig. 12 than in Fig. 10. The response around 180 Hz was notably reduced. There were no notable

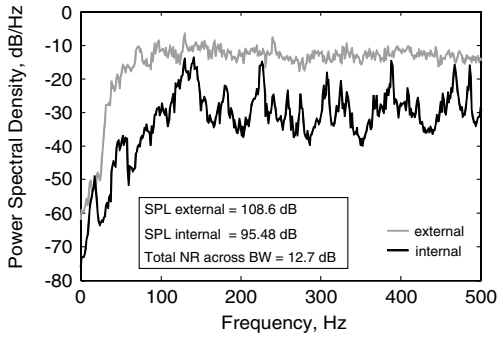

Fig. 10 External and internal noise levels for the bare cylinder (0–500 Hz).

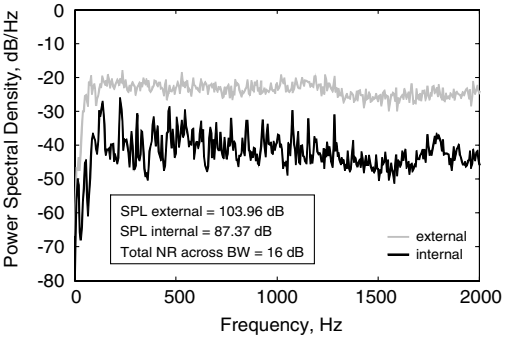

Fig. 13 External and internal responses with plugs added, but no acoustic dampers (0–2000 Hz).

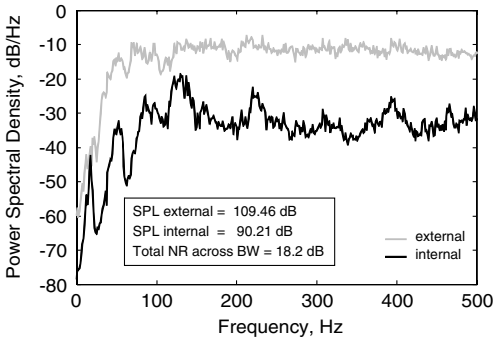

Fig. 14 External and internal responses with all acoustic dampers (0–500 Hz).

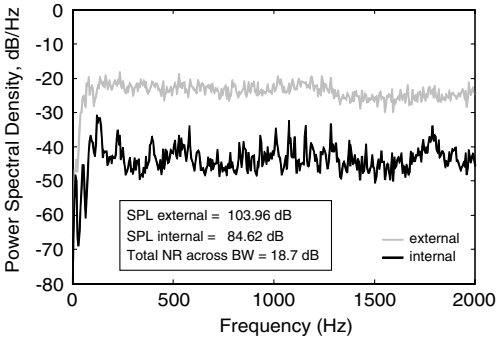

Fig. 15 External and internal responses with all acoustic dampers (0–2000 Hz).

differences between the internal response shown in Fig. 13 and that shown in Fig. 11.

The next tests demonstrate the performance with the acoustic dampers "active." Results are presented in Figs. 14 and 15. Overall, the noise reduction increased by 4.6 dB over the baseline measurement for the 500 Hz bandwidth, and 2.7 dB for the 2000 Hz bandwidth. Little impact was observed at peaks corresponding to structural resonances. Most reduction occurred above the first acoustic resonance. Although there was only modest reduction around 120 Hz (first acoustic resonance), modes above 200 Hz were very well attenuated. The measured reductions include: 6 dB at 120 Hz, 10 dB at 275 Hz, 12 dB at 225 Hz, 460 Hz, and 485 Hz, and 15 dB at 305 Hz. Figure 15 indicates that reduction was measured from the first acoustic resonance and up.

In the next series of tests, all resonator necks were blocked so that they were "inactive," and a 2.5 cm thick acoustic blanket (melamine) (1.22 kg) was attached to the interior cylinder wall. The results are presented in Figs. 16 and 17. Overall, the noise reduction increased (relative to the baseline) by 4.9 dB for the 500 Hz bandwidth, and 8.0 dB for the 2000 Hz bandwidth. As expected, the acoustic blanket performed well at higher frequencies (above 1000 Hz), and had a strong impact between 200 and 1000 Hz. Very little impact was observed at the first acoustic resonance and at frequencies below.

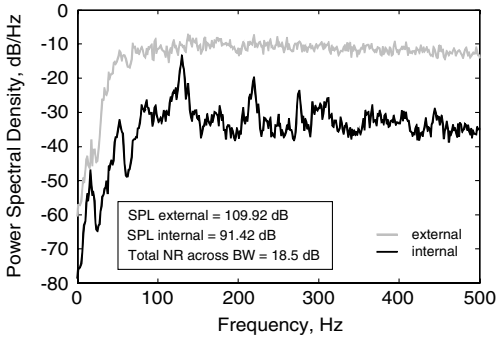

Fig. 16 External and internal responses with 2.5 cm acoustic blanket (0–500 Hz).

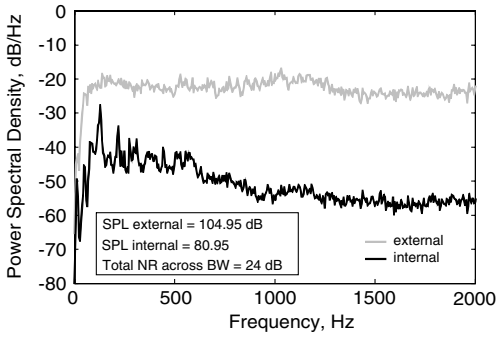

Fig. 17 External and internal responses with 2.5 cm acoustic blanket (0–2000 Hz).

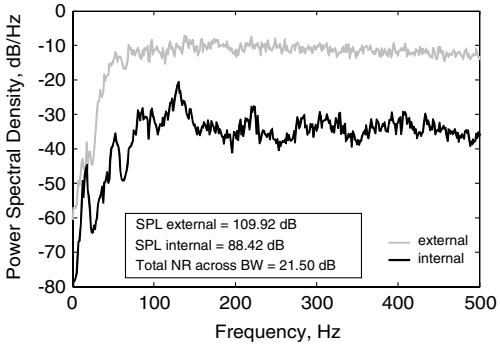

Fig. 18 External and internal responses using the acoustic blanket with the acoustic dampers (0–500 Hz).

The final series of tests show the performance of active acoustic dampers with the acoustic blanket treatment. The results are given in Figs. 18 and 19. Overall, the noise reduction increased by 7.9 dB for the 500 Hz bandwidth, and 10.3 dB for the 2000 Hz bandwidth, relative to the baseline. Comparing these results to the previous results indicates that the acoustic dampers provided an additional 3.0 dB (over the 500 Hz bandwidth) and 2.3 dB (over the 2000 Hz bandwidth), slightly less than the contribution of the dampers in Figs. 12 and 13. There were notable reductions at 55 Hz and around 90 Hz. Performance at the first acoustic resonance was much improved with the addition of the acoustic dampers. Performance above 700 Hz was very similar to that shown in Fig. 17, but there was obvious improvement below 700 Hz.

The noise reduction measurements for each case are summarized in Table 2 for both bandwidths. Note that for the low-frequency bandwidth, the noise reduction provided by the dampers was only about 0.3 dB less than that provided by the blanket. However, the blanket treatment had no beneficial impact on the fundamental acoustic resonance (120 Hz), whereas the dampers were able to provide some attenuation. The acoustic blanket provided significantly more noise reduction than the dampers over the 2000 Hz bandwidth.

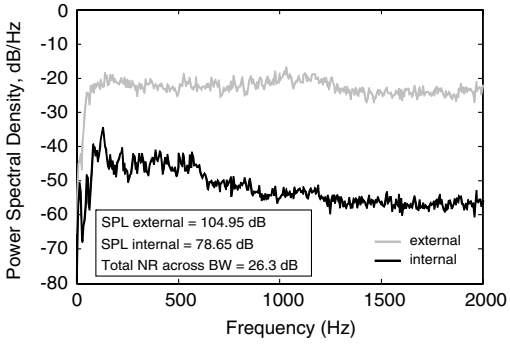

Fig. 19 External and internal responses using the acoustic blanket with the acoustic dampers (0–2000 Hz).

Table 2 Summary of noise reduction measurements

	0–500 Hz, dB	0–2000 Hz, dB
Bare	12.7	15.3
With plugs	13.6	16.0
Resonators	18.2	18.7
Acoustic blanket	18.5	24.0
Blanket and resonators	21.5	26.3

V. Conclusions

This work has discussed how the axial chambers of a composite chamber core structure might be used to augment acoustic blankets and attenuate low-frequency acoustic resonances in payload fairings. An empirical modeling approach was demonstrated that can be used to guide the design of acoustic dampers for a given fairing geometry. By designing multiple resonators to cover the low-frequency bandwidth, significant noise reduction was measured from the first acoustic mode up to approximately 700 Hz with virtually no added mass or reduction of usable payload volume, a tremendous advantage over equivalent blanket treatments or other acoustic mitigation devices.

Measurements on the bare chamber core cylinder revealed some important transmission phenomena. The interior acoustic response significantly increases starting at the fundamental acoustic resonance frequency. In fact, the overall low-frequency response (i.e., below 200 Hz) was dominated by the acoustic resonances of the enclosed volume. This indicates the importance of targeting acoustic resonances when trying to mitigate the vibroacoustic loads acting on payloads. The breathing mode of the cylinder that occurs when the volume is not airtight (which is always the case for real payload fairings) contributed to a strong transmission peak at low-frequency.

Measurements taken when using the axial tubes as acoustic dampers showed a reduction of approximately 4.6 dB over the 0–500 Hz bandwidth and 2.7 dB for the 2000 Hz bandwidth. Narrowband reductions were higher ($\sim$15 dB) near specific acoustic resonances. Almost all reduction was observed above the first acoustic resonance frequency. Although there was only modest reduction around 120 Hz (the first acoustic resonance), modes above 200 Hz were very well attenuated (i.e., more than 3 dB). In these tests, the resonators were designed to cover the bandwidth of 55 Hz up to about 2000 Hz. An improved approach for fairing applications would be to design the resonators to target only the bandwidth from the fundamental acoustic resonance up to about 500 Hz. Resonators below 120 Hz had very little contribution to the measured noise reduction.

For comparison purposes, measurements were taken using a 2.5 cm acoustic blanket treatment attached to the cylinder interior. As expected, the acoustic blanket performed very well at frequencies above 1000 Hz, and even had a strong impact between 200 and 1000 Hz. Very little impact was observed at the first acoustic resonance and at frequencies below. Neither the blanket nor acoustic dampers provided significant attenuation of the Helmholtz mode or the low-frequency structural modes.

Combining the acoustic resonators with the acoustic blanket treatment improved the noise reduction relative to the baseline measurements by 7.9 dB for the 500 Hz bandwidth, and 10.3 dB for the 2000 Hz bandwidth. The acoustic dampers provided an additional 3.0 dB (over the 500 Hz bandwidth) and 2.3 dB (over the 2000 Hz bandwidth) to the acoustic blanket performance. Comparing the results showed that the acoustic dampers provided some improvement up through 700 Hz. This demonstrates that chamber core fairings may offer significant contributions to mitigating low-frequency vibroacoustic loads and reducing the necessary mass and volume requirements of acoustic blanket treatments.

References

[1] Lane, S. A., Griffin, S., and Richard, R. E., "Fairing Noise Mitigation Using Passive Vibroacoustic Attenuation Devices," *Journal of Spacecraft and Rockets*, Vol. 43, No. 1, 2006, pp. 31–44.

[2] Kidner, M. R. F., Fuller, C. R., and Gardner, B., "Increase in Transmission Loss of Single Panels by Addition of Mass Inclusions to a Poro-Elastic Layer: Experimental Investigation," *Journal of Sound and Vibration*, Vol. 294, No. 3, 2006, pp. 466–472.

[3] Esteve, S. J., and Johnson, M. E., "Adaptive Helmholtz Resonators and Passive Vibration Absorbers for Cylinder Interior Noise Control," *Journal of Sound and Vibration*, Vol. 288, Nos. 4–5, 2005, pp. 1105–1130.

[4] Lane, S. A., Griffin, S., and Leo, D., "Active Structural Acoustic Control of a Launch Vehicle Fairing Using Monolithic Piezoceramic Actuators," *Journal of Intelligent Material Systems and Structures*, Vol. 12, No. 12, 2001, pp. 795–806.

[5] Lane, S. A., Kemp, J. D., Griffin, S., and Clark, R. L., "Active Acoustic Control of a Rocket Fairing Using Spatially Weighted Transducer Arrays," *Journal of Spacecraft and Rockets*, Vol. 38, No. 1, 2001, pp. 112–119.

[6] Lane, S. A., Johnson, M. E., Fuller, C. R., and Charpentier, A., "Active Control of Payload Fairing Noise," *Journal of Sound and Vibration*, Vol. 290, Nos. 3–5, 2006, pp. 794–819.

[7] Herup, E., Huybrechts, S., Griffin, S., and Tsai, S., U.S. Patent for "Method of Making Composite Chamber Core Sandwich-Type Structures with Inherent Acoustic Attenuation," Patent No. 6,213,710, 2001.

[8] George, T., Herman, S., Huybrechts, S., and Meink, T., "Optimal Design of Composite Chamber Core Structures," *Composite Structures*, Vol. 52, Nos. 3–4, 2001, pp. 277–286.

[9] Li, D., and Vipperman, J., "Noise Transmission Control Studies on a Chamber Core Composite Cylinder," IMECE Paper 03-41978, 2003.

[10] Henderson, B. K., Lane, S. A., Gerhart, C., and Richard, R. E., "Overview of the Vibro-Acoustic Launch Protection Experiment at the Air Force Research Laboratory," *Proceedings of SPIE–The International Society for Optical Engineering*, Vol. 5054, edited by Eric Anderson, Society of Photo-Optical Instrumentation Engineers (International Society for Optical Engineering), Bellingham, WA, 2003 pp. 66–72.

[11] Gerhart, C., Henderson, B. K., Griffin, S., Lazzaro, A., Evert, M., McCrary, W., and Ardelean, E., "The Vibro Acoustic Launch Protection Experiment Overview and Flight Results Summary," *Proceedings of SPIE–The International Society for Optical Engineering*, Vol. 5388, edited by Eric Anderson, Society of Photo–Optical Instrumentation Engineers (International Society for Optical Engineering), Bellingham, WA, 2004, pp. 43–52.

[12] Li, D. Y., and Vipperman, J. S., "On the Noise Transmission and Control for a Cylindrical Chamber Core Composite Structure," *Journal of Sound and Vibration*, Vol. 288, Nos. 1–2, 2005, pp. 235–254.

[13] Li, D., "Vibroacoustic Behavior and Noise Control Studies of Advanced Composite Structures," Ph.D. Dissertation, University of Pittsburgh, Pittsburgh, PA, 2003.

[14] Gardonio, P., Ferguson, N., and Fahy, F., "Modal Expansion Analysis of Noise Transmission Through Circular Cylindrical Shell Structure with Blocking Masses," *Journal of Sound and Vibration*, Vol. 244, No. 2, 2001, pp. 259–297.

[15] Crocker, M. (ed.), "Standing Waves," *Encyclopedia of Acoustics*, Vol. 1, Sec. 7, John Wiley & Sons, Inc., New York, 1997, pp. 81–89.

[16] Schofield, C., "An Investigation into the Acoustic Interaction Between a Helmholtz Resonator and a Room," Final-Year B.Sc. Project Report, Institute of Sound and Vibration Research, University of Southampton, 1979.

[17] Fahy, F. J., and Schofield, C., "A Note on the Interaction Between a Helmholtz Resonator and an Acoustic Mode of an Enclosure," *Journal of Sound and Vibration*, Vol. 72, No. 3, 1980, pp. 365–378.

[18] Cummings, A., "The Effect of a Resonator Array on the Sound Field in a Cavity," *Journal of Sound and Vibration*, Vol. 154, No. 1, 1992, pp. 25–44.

[19] Lane, S., Richard, R., and Kennedy, S., "Fairing Noise Control Using Tube-Shaped Resonators," *Journal of Spacecraft and Rockets*, Vol. 42, No. 4, 2005, pp. 640–646.

[20] Bies, D. A., and Hansen, C. H., *Engineering Noise Control, Theory and Practice*, 2nd ed., E&FN Spon, New York, 1996, p. 282.

[21] Bies, D. A., and Hansen, C. H., *Engineering Noise Control, Theory and Practice*, 2nd ed., E&FN Spon, New York, 1996, p. 279.

[22] MATLAB Software, Release 13, The Math Works, Natick, MA, 2004.

L. Peterson
Associate Editor